

A Proposal-Based Solution to Spatio-Temporal Action Detection in Untrimmed Videos

Joshua Gleason*, Rajeev Ranjan*, Steven Schwarcz*, Carlos D. Castillo, Jun-Cheng Chen,
Rama Chellappa
University of Maryland, College Park

gleason@umiacs.umd.edu, rranjan1@umiacs.umd.edu, schwarcz@umiacs.umd.edu

*these authors contributed equally to this work

Abstract

Existing approaches for spatio-temporal action detection in videos are limited by the spatial extent and temporal duration of the actions. In this paper, we present a modular system for spatio-temporal action detection in untrimmed security videos. We propose a two stage approach. The first stage generates dense spatio-temporal proposals using hierarchical clustering and temporal jittering techniques on frame-wise object detections. The second stage is a Temporal Refinement I3D (TRI-3D) network that performs action classification and temporal refinement on the generated proposals. The object detection-based proposal generation step helps in detecting actions occurring in a small spatial region of a video frame, while temporal jittering and refinement helps in detecting actions of variable lengths. Experimental results on the spatio-temporal action detection dataset - DIVA - show the effectiveness of our system. For comparison, the performance of our system is also evaluated on the THUMOS'14 temporal action detection dataset.

1. Introduction

Action detection in untrimmed videos is a challenging problem. Although methods using deep convolutional neural networks (CNNs) have significantly improved performance on action classification, they still struggle to achieve precise spatio-temporal action localization in challenging security videos. There are some major challenges associated with action detection from untrimmed security videos. First, the action typically occurs in a small spatial region relative to the entire video frame. This makes it difficult to detect the actors/objects involved in the action. Second, the duration of the action may vary significantly, ranging from a couple of seconds to a few minutes. This requires the detection procedure to be robust to temporal variation. Existing publicly available action detection datasets such as THUMOS'14 [20] and AVA [15] do not possess these challenges. Hence, algorithms trained on these datasets have

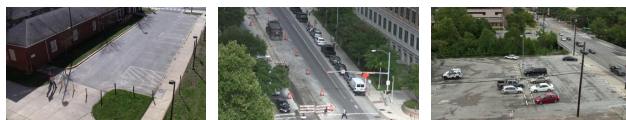


Figure 1. Sample images of different scenes of the DIVA dataset which presents challenging action detection scenarios which require algorithms to be robust to large variations in scale, object pose, and camera viewpoint.

sub-optimal performance on untrimmed security videos. In this paper, we work with the DIVA dataset that has untrimmed security videos. Videos that comprise the DIVA dataset are a subset of those in the VIRAT dataset [34], albeit with newly introduced annotations that make them suitable for the activity detection task. Figure 1 shows some sample frames from the DIVA dataset.

In this work we introduce a proposal-based modular system for performing spatio-temporal action detection in untrimmed videos. Our system generates spatio-temporal action proposals based on detections from an off-the-shelf detector, then classifies the proposals using an existing network architecture with minor changes.

Our proposed system has the advantage that it is both simple and does not require tracking of moving objects. Tracking of objects, often seen as an important component in action recognition systems, presents considerable challenges. Tracking errors generate problems in action recognition from which it is very difficult to recover. On the other hand, object detection has advanced consistently over the past few years, with more sophisticated frame-wise object detectors becoming available. These detectors can be successfully applied to previously unseen videos.

The proposed approach for action detection is based on the observation that we can generate high-recall proposals by clustering object detections. The dense proposals are then applied to a deep 3D-CNN to classify them as either one of the action classes or the non-action class. The temporal bounds for the proposals are also refined to improve



Figure 2. Sample frames of some activities of the DIVA dataset.

localization. We modify the existing I3D [5] network for action classification by adding an additional loss term for temporal refinement. We call the modified network Temporal Refinement I3D (TRI-3D). In summary, this paper makes the following contributions:

- We introduce a proposal-based modular system for spatio-temporal action detection in untrimmed security videos.
- We propose an algorithm using hierarchical clustering and temporal jittering for generating action proposals using frame-wise object detections.
- We propose the Temporal Refinement I3D (TRI-3D) network for action classification and temporal localization.
- We evaluate our system on the DIVA dataset, which is an untrimmed security video dataset in the wild.

2. Related Work

Much research has gone into designing algorithms for action classification from videos. In recent years, many methods have achieved remarkable performance using CNNs for the task of action classification [43, 25, 31, 51]. While [25, 51] use frame-based features, [43] uses a two-stream (RGB and optical-flow) CNN approach to utilize the temporal information of videos. More recently, researchers have used 3D-CNNs for action classification [5, 44, 17, 39] that simultaneously take in multiple video frames and classify them into actions.

The task of spatio-temporal action detection from untrimmed videos is a challenging problem. Less work has gone into localizing actions, not just along the temporal axis but also in terms of spatial localization. Existing action detection algorithms can be broadly classified into 1) end-to-end systems, and 2) proposal-based systems. The end-to-end action detection approaches feed a chunk of video frames into a CNN which simultaneously classifies and localizes the action. Hou et al. [17] proposed a tube convolutional neural network (T-CNN) that generates tube proposals from video-clips and performs action classification and localization using an end-to-end 3D-CNN. Kalogeiton et al. [23] extracts convolutional features from each frame of a video, and stacks them to learn spatial locations and action scores. Although these end-to-end learning methods may have a simpler pipeline, they are less effective for security videos, where the action is likely to happen in a small spatial region of a frame. On the other hand, proposal-based methods perform action detection in two steps. The

first step computes the action proposals, while the second step classifies and localizes the action. Some proposal-based methods are presented in [35, 54, 29, 14, 28]. Unlike existing proposal-based approaches, our method uses hierarchical clustering and temporal jittering to group frame-wise object detections obtained from off-the-shelf detectors in the spatio-temporal domain. It gives us the advantage of detecting variable length action sequences spanning a small spatial region of the video.

In this section we have covered a number of action recognition works, however this list is far from complete. For further action recognition works we point the reader to a more extensive curated list presented in [7].

3. DIVA dataset

The DIVA dataset is a new spatio-temporal action detection dataset for untrimmed videos. While we present our work on the DIVA dataset, and there are currently no other papers we can cite that reference the DIVA dataset at this time, we would like to emphasize that we did not create the DIVA dataset, nor are we the only ones who have access to it. We would like to point out that a workshop on DIVA results will be organized as part of WACV 2019. The current release of the DIVA dataset (DIVA V1) is adapted from the VIRAT dataset [34] with new annotations for 12 simple and complex actions of interest focusing on the public security domain. All actions involve either people or vehicles. Actions include vehicle U-turn, vehicle left-turn, vehicle right turn, closing trunk, opening trunk, loading, unloading, transport heavy carry, open (door), close (door), enter, and exit. The dataset currently consists of 455 video clips with 12 hours and 40 minutes in total captured at different sites. There are 64 videos in the training set, 54 videos in the validation set, 96 videos with annotations withheld in the test set. The remaining videos are for future versions of the dataset. All video resolutions are either 1200×720 or 1920×1080 and humans range in height from 20 to 180 pixels. We show sample images of different scenes and sample frames of some activities in Figure 1 and Figure 2 respectively. In addition, the number of training instances per action is shown in Figure 3.

3.1. Challenges

As compared to other action detection datasets, such as the THUMOS'14 [20] and AVA [15] datasets, the DIVA dataset introduces several new challenges for the action detection task that make methods designed for existing action

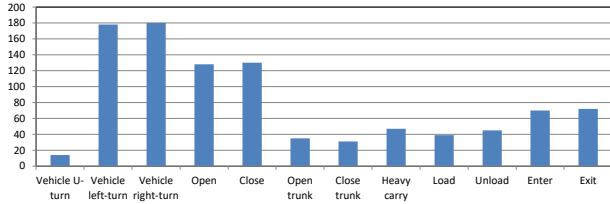


Figure 3. The number of training instances per action from the DIVA training set.

datasets unsuitable. The first issue is the sparsity of actions, both spatially and temporally. For example, exactly half of all videos contain at least 30 seconds of footage where no actions are performed. What makes DIVA particularly challenging is the spatial sparsity of actions: the average size for the bounding boxes of all actions in the training set is 264×142 . As a result, when an action is occurring it only takes up on average less than 2.6% of the pixels in any given image, and no action in the entire dataset takes up more than 40%. Additionally, with few exceptions, the similarity of each action and each environment makes it very difficult to use the context of the surrounding scene to assist in classification.

When compared with other setups, where actions are assumed to make up the majority of pixels on any given frame, this motivates the need for a completely different approach focused on the localization of activities. For example, [37] mention that the smallest anchor size in Faster-RCNN is 128×128 on a 600×600 input image, or 4.5% of the image pixels. This means the average action in DIVA is barely more than half the size of the smallest object detectable by conventional means.

The dataset also contains significant spatial and temporal overlap between activities. This is not just an issue between unrelated activities in the same frame (*e.g.* one person entering a car while another leaves a different car), but is actually more fundamental. For a common example, consider the activities `opening`, `entering`, and `closing`, which apply to a human actor interacting with a car. In order to enter a car, a subject may first open the car door (though it may already be open), and will often close it afterwards (though they may not). All three of these actions are usually performed in quick succession, yet DIVA begins annotation of each activity one second before it begins, and finishes annotating one second after it completes. It is therefore imperative that our system can handle large degrees of spatio-temporal overlap.

4. Proposed Approach

Our approach consists of three distinct modules. The first one generates class-independent spatio-temporal proposals from a given untrimmed video sequence. The second module performs action classification and temporal localization on these generated proposals using a deep 3D-CNN. The final module is a post-processing step that performs 3D



Figure 4. On the left, the DIVA action `Closing` makes up only a small portion of the image, and the surrounding context has no value for the action classification task. The THUMOS action `Cricket` on the right is much larger in the image, and the entire image’s context is useful for classification.



Figure 5. Some of object detection and segmentation results for the DIVA dataset using Mask-RCNN [16].

non-maximum suppression (NMS) for precise action detection. The system diagram for our approach is shown in Figure 6. In the following sub-sections we discuss in detail the steps of our proposed approach.

4.1. Action Proposal Generation

The primary goal of the action proposal generation stage is to produce spatio-temporal cuboids from a video with high recall and little regard for precision. Although sliding-window search in spatio-temporal space is a viable method for proposal generation, it is computationally very expensive. An alternate solution is to use unsupervised methods to cluster the spatio-temporal regions from a video in a meaningful way. In our approach, we generate the action proposals by grouping frame-wise object detections obtained from Mask-RCNN [16] in the spatio-temporal domain using hierarchical clustering. These generated proposals are further jittered temporally to increase the overall recall.

4.1.1 Object Detection

For object detection, we apply Mask R-CNN [16], an extension of the well-known Faster R-CNN [37] framework. In addition to the original classification and bounding box regression network of Faster R-CNN, Mask-RCNN adds another branch to predict segmentation masks for each Region of Interest (RoI). In Figure 5, we show some sample results from video frames of the DIVA dataset. We observe that Mask-RCNN is able to detect humans and vehicles at different scales, a feature which is useful for detecting the multi-scale actions of the DIVA datasets.

4.1.2 Hierarchical Clustering

The objects detected using Mask-RCNN are represented by a 3-dimensional feature vector (x, y, f) , where (x, y) denotes the center of the object bounding box and f denotes

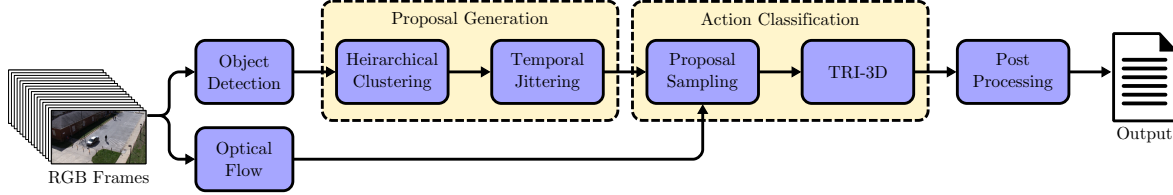


Figure 6. Proposed system for spatio-temporal action detection.

the frame number. We use the SciPy implementation of Divisive Hierarchical Clustering [30, 21] to generate clusters from the 3-dimensional features. We dynamically split the resulting linkage tree at various levels to create k clusters, where k is proportional of video length. The proposals are generated from the bounding box of all detections in the cluster. They are cuboids in space-time and are denoted by $(x_{min}, y_{min}, x_{max}, y_{max}, f_{start}, f_{end})$. This yields an average of approximately 250 action proposals per video on DIVA validation set. Further details regarding the exact implementation can be found in the supplementary material.

4.1.3 Dense Action Proposals with Temporal Jittering

Although the proposals generated using hierarchical clustering reduce the spatio-temporal search space for action detection, they are unable to generate high recall for the following two reasons: 1) The generated proposals are independent of both the action class and cuboid temporal bounds. Hence, they are less likely to overlap precisely with the ground-truth action bounds. 2) Few proposals are generated. A higher recall is achieved with larger numbers of proposals. In order to solve these issues, we propose a temporal jittering approach to generate dense action proposals from the existing proposals obtained from hierarchical clustering.

Let the start and end frames for an existing proposal be denoted by f_{st} and f_{end} respectively. We first choose the anchor frames by sliding along the temporal axis from f_{st} to f_{end} with a stride of s . The anchor frames thus selected

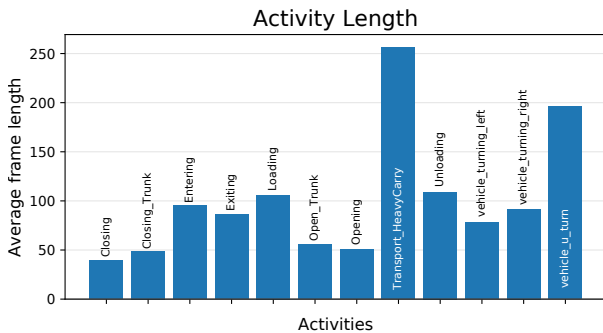


Figure 7. The average frame lengths for 12 different activities from the DIVA training set.

are $(f_{st}, f_{st} + s, f_{st} + 2s, f_{st} + 3s, \dots, f_{end})$. For each of the anchor frames f_a , we generate four sets of proposals with temporal bounds $(f_a - 16, f_a + 16)$, $(f_a - 32, f_a +$

$32)$, $(f_a - 64, f_a + 64)$ and $(f_a - 128, f_a + 128)$. We choose the proposals frame lengths to be $\{32, 64, 128, 256\}$ based on the average frame lengths for the actions in the DIVA dataset which range between 32 – 256 (see Figure 7). The pseudo-code for generating dense action proposals is presented in Algorithm 1.

Algorithm 1 Dense Proposal Generation

```

1: detections  $\leftarrow$  Mask-RCNN(video)
2: orig_proposals  $\leftarrow$  hierarchical_clustering(detections)
3: new_proposals  $\leftarrow$  orig_proposals
4: s  $\leftarrow$  15
5: for proposal in orig_proposals do
6:    $x_0, y_0, x_1, y_1 \leftarrow$  spatial_bounds(proposal)
7:    $f_{st}, f_{end} \leftarrow$  temporal_bounds(proposal)
8:   for  $f$  from  $f_{st}$  to  $f_{end}$  step  $s$  do
9:     new_proposals.add( $f - 16, f + 16$ )
10:    new_proposals.add( $f - 32, f + 32$ )
11:    new_proposals.add( $f - 64, f + 64$ )
12:    new_proposals.add( $f - 128, f + 128$ )
13: final_dense_proposals  $\leftarrow$  new_proposals

```

Generating dense proposals using temporal jittering has two advantages. First, the recall is higher. Second, having a large number of dense training proposals provides better data augmentation for training, thus improving performance.

Figure 8 provides a quantitative comparison of three action proposal generation methods on the DIVA validation set in terms of recall vs 3D Intersection over Union (IoU) with the ground-truth activities: 1) Rule based 2) Hierar-

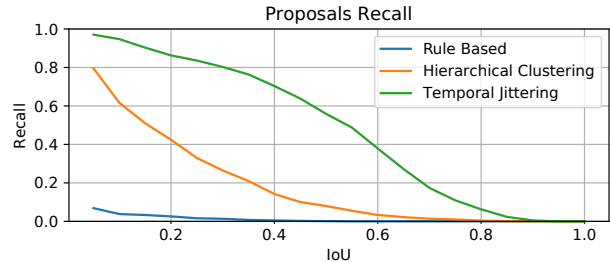


Figure 8. The recall for different action-proposal generation methods as a function of spatio-temporal intersection over union (IoU) overlap on the DIVA validation set.

chical clustering, and 3) Temporal Jittering. The rule based proposal generation method uses hand-crafted rules to as-

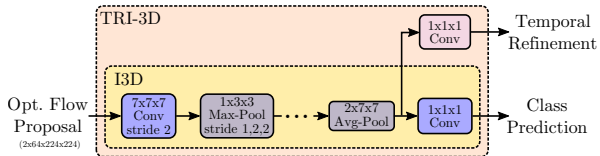


Figure 9. TRI-3D network. For details on the I3D please refer to Figure 3 in [5].

sociate detections across consecutive frames. For example, a rule stating “a person detection and a car detection closer than 50 pixels is a proposal” can be used to generate action proposals using Prolog. However, the recall with our rule based proposal generation method is poor. On the other hand, hierarchical clustering provides 40% recall at a spatio-temporal IoU of 0.2. Using temporal jittering on top of it increases the recall to 85%. This shows the effectiveness of our dense proposal generation method.

4.2. Action Proposal Refinement and Classification

The proposal refinement and classification step takes in the generated dense proposals as input and performs the following tasks:

- Identify the non-action proposals.
- Identify the action proposals and classify them into one of the given action classes.
- Improve the temporal localization of the action proposals by refining their temporal bounds.

To accomplish these tasks we begin with the I3D network architecture [10] which classifies each proposal cuboid as one of the 12 action classes or as a non-action class. Due to the sparsity of action proposals, many of the ground truth actions don’t perfectly correspond to any of the action proposals. To mitigate this issue, a regression objective is added to the final layer of I3D to predict a temporal correction to the cuboid. This defines the TRI-3D network. Figure 9 depicts the network architecture of the proposed TRI-3D. A detailed description of input pre-processing and the working of TRI-3D is provided in the following subsections.

4.2.1 Input Pre-processing

The input to the TRI-3D network is $64 \times 224 \times 224$ optical flow frames which are computed using the TV-L1 optical flow algorithm [52]. The original I3D is designed for full sized frames on the Kinetics dataset. It first scales the input videos so that the smallest dimension is equal to 256, then samples a random 224×224 crop during training. Unlike the Kinetics dataset, the aspect ratio of generated dense proposal cuboids is arbitrary. To address this issue we pad the smaller side of the proposal relative to the center so that it is the same size as the largest side prior to sampling the optical flow data. This has the potential to add a significant amount of extra padding to proposal cuboids that have a significant

discrepancy between the dimensions; however, more conservative padding and cropping schemes performed poorly during preliminary testing (Section 5.2).

A proposal may also extend across an arbitrary number of frames. However, since I3D requires a fixed number of input frames, we chose to uniformly sample the fixed number of frames across the temporal span of each proposal as shown in Figure 10. This strategy follows the original I3D work in many cases. The sampling strategy differs from the original work when the total number of frames in a proposal is less than 64. In this scenario, instead of wrapping the sampling we continue to sample uniformly, potentially sampling the same frame multiple times in a row. This strategy ensures frames are always provided to the network in temporally increasing order which is necessary for temporal refinement.

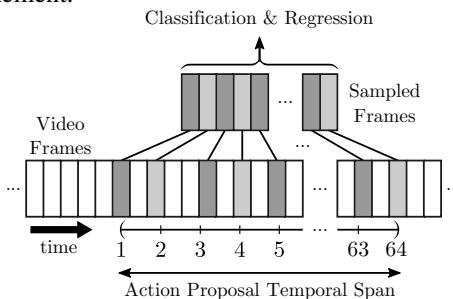


Figure 10. Uniform sampling 64 input frames from an arbitrarily long action proposal.

After sampling the cropped cuboid from the optical flow video, the sample is then resized to 256×256 . During training we randomly sample a 224×224 crop from the cuboid.

To improve the robustness of the network we apply random horizontal flips on all training examples except the non-symmetric actions: `vehicle turning left`, `vehicle turning right`, and `vehicle u turn`.

The TRI-3D network uses optical flow frames as input. The two-stream I3D network has been shown to outperform the single stream network on the Kinetics dataset, however through experimentation we discovered that the two-stream network performed worse for overall prediction accuracy when using the ground truth actions, which motivated our choice to use only optical flow, see Section 5.2. An additional benefit of this choice is an improvement in classification speed.

Since the videos in the dataset are from stationary cameras we don’t perform any normalizations to the optical flow to adjust the mean value.

4.2.2 TRI-3D Training

The target data for the TRI-3D network is derived from proposals generated from training data and labeled from ground truth annotations. We label each proposal produced by the proposal generator as either one of the action classes or the non-action class. If a proposal is found to have a

sufficient IoU overlap with a ground truth annotation, then a temporal refinement value is also calculated. A proposal with spatial IoU above 0.35 and temporal IoU above 0.5 with the ground-truth is designated as a “positive” proposal and assigned an action class label. A proposal with temporal IoU less than 0.2 is designated as a “negative” proposal. Negative proposals are further separated into two designations, easy negatives and hard negatives. Any negative proposal with spatial IoU above 0.35 and temporal IoU between 0.01 and 0.2 with ground truth is a hard negative, and the remaining negatives are easy negatives.

In order to improve the robustness of our network with respect to false alarms we construct our training data using all of the proposals which were assigned a class label, as well as all of the hard negatives. A total of 9,525 easy negatives are generated, however most of the easy negatives are omitted from the training data. The only easy negatives used are those which result from hierarchical clustering, omitting those derived from temporal jittering. The total number of training examples for each designation are shown in Table 1

Positive	Easy Neg.	Hard Neg.	Total
12,752	9,525	13,574	35,851

Table 1. Numbers of proposals of each type used during training of our TRI-3D network.

The number of training samples generated for different action classes vary widely. For instance, the number of positive samples for `vehicle u turn` is 215, while it’s 2,554 for `vehicle right turn`. To mitigate the effect of the high class imbalance, we duplicate the positive instances of each class such that all the action classes have an equal number of positive samples during training. This helps the network to learn equally discriminative features for all the action classes involved in training.

4.2.3 TRI-3D Loss Functions

The TRI-3D network takes in the preprocessed proposals and performs action classification as well as temporal refinement. For training action classification, we use a multi-class cross-entropy loss function L_{cls} as shown in (1)

$$L_{cls} = \sum_{a=0}^{12} -y_a \cdot \log(p_a), \quad (1)$$

where $y_a = 1$ if the sample belongs to class a , otherwise 0. The predicted probability that a sample belongs to class a is given by p_a . The 12 action classes are labeled from $a = 1$ to $a = 12$, while the non-action class is labeled $a = 0$.

We also refine the temporal bounds of the proposals by adjusting its start and end frames according to the predicted regression values. Let the start and end frames for the input proposal and the ground-truth be (f_{st}, f_{end}) and $(\hat{f}_{st}, \hat{f}_{end})$, respectively. We select the mid-frame of the proposal as $f_a = (f_{st} + f_{end})/2$, and the half-length of the

proposal as $t = (f_{end} - f_{st} + 1)/2$. The normalized ground truth regression pair is generated by (2):

$$(r_{st}, r_{end}) = \left(\frac{\hat{f}_{st} - f_a}{t}, \frac{\hat{f}_{end} - f_a}{t} \right). \quad (2)$$

We use the smooth_{L1} loss [37] to generate the regression outputs $v = (v_{st}, v_{end})$ for the ground-truth labels $r = (r_{st}, r_{end})$, as shown in (3)

$$L_{loc}(v, r) = \text{smooth}_{L1}(r_{st} - v_{st}) + \text{smooth}_{L1}(r_{end} - v_{end}), \quad (3)$$

in which

$$\text{smooth}_{L1}(x) = \begin{cases} 0.5x^2 & \text{if } |x| < 1 \\ |x| - 0.5 & \text{otherwise.} \end{cases} \quad (4)$$

We combine the action classification and the temporal regression loss in a multi-task fashion as given by (5)

$$L_{full} = L_{cls} + \lambda[a \geq 1]L_{loc}, \quad (5)$$

where λ is chosen to be 0.25. The temporal refinement loss is activated only for the positive proposals that belong to one of the 12 action classes ($a \geq 1$). For a non-class proposal, the temporal refinement loss doesn’t generate any gradients. We train the TRI-3D network using the Adam [26] optimization technique, with initial learning rate set to 0.0005.

4.3. Post-processing

At test time, the TRI-3D network outputs the classification score and the refined temporal bounds for an input proposal. Our method for proposal generation creates many highly-overlapping action proposals, many of which are classified as the same class. We prune overlapping cuboids using 3D-NMS. The 3D-NMS algorithm is applied to each of the classes separately and considers two proposals to be overlapping when the temporal IoU overlap is greater than 0.2 and the spatial IoU overlap is greater than 0.05.

5. Experimental Evaluation

In this section we present and discuss various experiments which motivate our design choices and describe the overall system performance. All experimental results are reported on the DIVA validation dataset unless otherwise indicated.

5.1. DIVA Evaluation Metric

To correctly and objectively assess the performance of the proposed action detection (AD) framework on DIVA, we adopt the measure: probability of missed detection P_{miss} at fixed rate of false alarm per minute $Rate_{FA}$, which is used in the surveillance event detection framework of TRECVID 2017 [33]. This metric evaluates whether the algorithm correctly detects the presence of the target action instances. A one-to-one correspondence from detection to ground-truth is enforced using the Hungarian algorithm, thus each detected action may be paired with either

Net Arch.	Input Mode	Pretrained	Crop	Acc
I3D	opt. flow	True	square	0.716
I3D	RGB	True	square	0.585
I3D	RGB+flow	True	square	0.704

Table 2. Classification accuracy for the preliminary classifier study on ground truth proposals from the DIVA validation set. The first row represents our final design. Subsequent rows contain experimental results with various modifications.

one or zero ground-truth actions. Any detected action which doesn’t correspond to a ground-truth action is a false alarm, and any ground-truth action which isn’t paired with a corresponding detection is a miss. The evaluation tool used in this work is available on Github [22]. For details of the evaluation metric we refer the reader to TRECVID 2017 [33].

5.2. Preliminary Classification Experiments

While developing our classification system we performed a number of preliminary experiments. The results of these experiments were used to justify the choices of network architecture, cropping scheme, and input modality. The experiments were performed by training on cuboids derived from ground truth annotations. Classification accuracy is reported on the DIVA validation ground truth cuboids.

The results of some of these experiments are shown in Table 2. One of the most surprising results was the discovery that the “single-stream” optical flow I3D network outperformed the two-stream I3D network. This is surprising because for other action recognition datasets two-stream networks generally outperform single stream networks [43, 10]. The output of the two-stream I3D network is computed by averaging the logits of the optical flow and RGB networks, which are trained independently. The table shows that the RGB I3D network is 13% less accurate than the optical flow network. The poor performance of the two-stream network appears to be due to the poor performance of the RGB I3D network.

Further experiments to motivate our choice of architecture and cropping scheme were performed and can be found in the Supplementary Material.

5.3. System Performance

In this section we present our experiments and results for the entire system. The primary goal of the system is to take untrimmed videos as input and report the frames where actions are taking place. We perform the following experiments in order to gain a better understanding of the system performance, to discover how much impact further improvements to proposal generation may have, and how much error is simply due to improper classification.

- *Action detection (AD)*: This is the primary task of the system. Given an untrimmed video, detect and classify the begin and end frame of each action.

- *AD with temporal reference segmentation (TRS)*: Perform the AD task but with additional temporal reference segmentation, that is, our system is provided the beginning and ending frames of each ground truth action, but not the class or spatial bounds.
- *AD with cuboid reference segmentation (CRS)*: Perform the AD task with both spatial and temporal reference segmentation. In this experiment the system is provided both the start and end frame of each activity as well as the spatial cuboid bounds for each activity.

In order to perform the TRS experiment we add an additional processing step between proposal generation and classification. We adjust the temporal bounds of any proposal which temporally overlaps a reference action. If a proposal overlaps multiple reference actions then multiple copies of the proposal are generated and the temporal bounds of the copies are adjusted to match each of the reference actions. Any proposals which have no temporal overlap with any reference actions are omitted. For this experiment we did not retrain the network and the temporal refinement values are ignored.

The CRS experiment is effectively performing action classification on reference cuboids. This is the same as the preliminary experiments described in Section 5.2. The results described here correspond to the experiment referred to in the first row of Table 2.

The results of the experiments are shown in Figure 11. From these figures we see that there is a high degree of performance variation among different classes. For the AD task the worst performing class at $Rate_{FA}$ of 0.1 is Transport Heavy Carry with P_{miss} of 0.935 and the best performing class is vehicle u-turn with a P_{miss} of 0.25. However, we see that at $Rate_{FA}$ of 0.01 the vehicle u-turn becomes the worst performing action. This appears to be due to the fact that very few training and validation examples are available.

The aggregated results described in Figure 11, and equivalently in Table 3, show the significant improvement gained by providing temporal reference segmentation. Surprisingly, only a small average improvement is observed when providing the cuboid reference segmentation.

DIVA Test Data: The DIVA test dataset annotations are unavailable to the authors at the time of writing this manuscript. We submitted a single set of results from our system for independent evaluation and have included these results as well as results from other performers on the DIVA dataset in Table 4. We have also included results from a publicly available implementation based on [46]. We keep the identities of other performers anonymous.

THUMOS’14 Dataset: In order to compare to other action detection systems we also evaluated on the Temporal Action Detection task of THUMOS’14 [20]. The THUMOS’14 Temporal Action Detection dataset contains 200

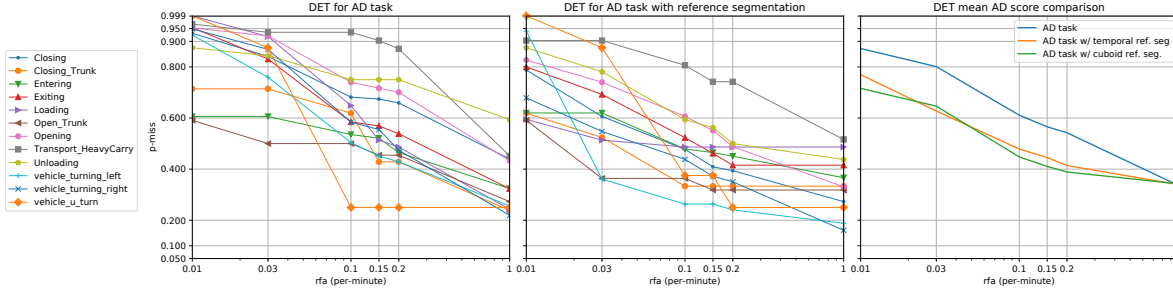


Figure 11. The left plot shows the per-class DET curves for the AD task. The center plot shows the per-class DET curves for TRS. The right plot shows the aggregated DET performance on the AD task compared to TRS and CRS.

$Rate_{FA}$	0.01	0.03	0.1	0.15	0.2	1.0
AD	0.870	0.800	0.610	0.563	0.542	0.361
Temporal Ref.	0.770	0.627	0.479	0.445	0.414	0.340
Cuboid Ref.	0.716	0.646	0.448	0.410	0.389	0.342

Table 3. Our system’s mean P_{miss} at fixed $Rate_{FA}$ on DIVA validation data. These are the values represented in the right plot in Figure 11.

R_{FA}	Xu <i>et al.</i> [46]	P4	P3	P2	P1	Ours
0.15	0.863	0.872	0.759	0.624	0.710	0.618
1.0	0.720	0.704	0.624	0.621	0.603	0.441

Table 4. Mean P_{miss} versus $Rate_{FA}$ on the DIVA test data for AD task obtained via independent evaluation. DIVA performers (P1-P4) and algorithms other than the baseline [46] have been kept anonymous by request of the independent evaluator. Only the performers better than the baseline are represented here (sorted by mean P_{miss} at $Rate_{FA}$ of 1). A lower P_{miss} value indicates superior performance, and the best performance is indicated in bold.

annotated validation videos, and 213 annotated test videos for 20 action classes. Since the THUMOS’14 dataset is fundamentally different from DIVA in that actions generally span the majority of the frame, we omit the hierarchical clustering phase and instead perform temporal jittering on the cuboid spanning the entire video.

Following common practice, we trained THUMOS’14 using the validation data for 5 epochs and then evaluated on the test data. The results are shown in Table 5. From this table we see that our system, while not designed for videos of this nature, performs well compared to state-of-the-art methods.

6. Conclusion

In this work we introduced an action detection system capable of handling arbitrary length actions in untrimmed security video on the difficult DIVA dataset. The system presented in this work is easily adapted to the THUMOS dataset. This system also leaves room for improvement and the modular design allows for easy integration of such future improvements. Although the DIVA evaluation metrics also includes an action-object detection task we choose to omit evaluation on this metric since our system doesn’t explicitly provide object level localization of activities. We leave such improvements and extensions to future work.

tIoU	0.1	0.2	0.3	0.4	0.5	0.6	0.7
Karaman <i>et al.</i> [24]	4.6	3.4	2.4	1.4	0.9	-	-
Oneata <i>et al.</i> [36]	36.6	33.6	27.0	20.8	14.4	-	-
Wang <i>et al.</i> [45]	18.2	17.0	14.0	11.7	8.3	-	-
Caba <i>et al.</i> [4]	-	-	-	-	13.5	-	-
Richard <i>et al.</i> [38]	39.7	35.7	30.0	23.2	15.2	-	-
Shou <i>et al.</i> [42]	47.7	43.5	36.3	28.7	19.0	10.3	5.3
Yeung <i>et al.</i> [48]	48.9	44.0	36.0	26.4	17.1	-	-
Yuan <i>et al.</i> [49]	51.4	42.6	33.6	26.1	18.8	-	-
Escorcía <i>et al.</i> [9]	-	-	-	-	13.9	-	-
Buch <i>et al.</i> [3]	-	-	37.8	-	23.0	-	-
Shou <i>et al.</i> [40]	-	-	40.1	29.4	23.3	13.1	7.9
Yuan <i>et al.</i> [50]	51.0	45.2	36.5	27.8	17.8	-	-
Buch <i>et al.</i> [2]	-	-	45.7	-	29.2	-	9.6
Gao <i>et al.</i> [12]	60.1	56.7	50.1	41.3	31.0	19.1	9.9
Hou <i>et al.</i> [18]	51.3	-	43.7	-	22.0	-	-
Dai <i>et al.</i> [8]	-	-	-	33.3	25.6	15.9	9.0
Gao <i>et al.</i> [13]	54.0	50.9	44.1	34.9	25.6	-	-
Xu <i>et al.</i> [46]	54.5	51.5	44.8	35.6	28.9	-	-
Zhao <i>et al.</i> [53]	60.3	56.2	50.6	40.8	29.1	-	-
Huang <i>et al.</i> [19]	-	-	-	-	27.7	-	-
Yang <i>et al.</i> [47]	-	-	44.1	37.1	28.2	20.6	12.7
Chao <i>et al.</i> [6]	59.8	57.1	53.2	48.5	42.8	33.8	20.8
Nguyen <i>et al.</i> [32]	52.0	44.7	35.5	25.8	16.9	9.9	4.3
Alwassel <i>et al.</i> [1]	-	-	51.8	42.4	30.8	20.2	11.1
Gao <i>et al.</i> [11]	-	-	-	-	29.9	-	-
Lin <i>et al.</i> [27]	-	-	53.5	45.0	36.9	28.4	20.0
Shou <i>et al.</i> [41]	-	-	35.8	29.0	21.2	13.4	5.8
Ours	52.1	51.4	49.7	46.1	37.4	26.2	15.2

Table 5. Comparison to THUMOS’14 performers on the mAP metric at various temporal IoUs. Missing entries indicate that results are not available. We note that Xu *et al.* [46] is the same system used to compute the DIVA V1 baseline; see Table 4. The best performance at each tIoU is indicated in bold.

Acknowledgments

This research is based upon work supported by the Office of the Director of National Intelligence (ODNI), Intelligence Advanced Research Projects Activity (IARPA), via IARPA R&D Contract No. D17PC00345. The views and conclusions contained herein are those of the authors and should not be interpreted as necessarily representing the official policies or endorsements, either expressed or implied, of ODNI, IARPA, or the U.S. Government. The U.S. Government is authorized to reproduce and distribute reprints for Governmental purposes notwithstanding any copyright annotation thereon.

References

- [1] H. Alwassel, F. Caba Heilbron, and B. Ghanem. Action search: Spotting actions in videos and its application to temporal action localization. In *The European Conference on Computer Vision (ECCV)*, 2018.
- [2] S. Buch, V. Escorcia, B. Ghanem, L. Fei-Fei, and J. Niebles. End-to-end, single-stream temporal action detection in untrimmed videos. In *Proceedings of the British Machine Vision Conference (BMVC)*, 2017.
- [3] S. Buch, V. Escorcia, C. Shen, B. Ghanem, and J. C. Niebles. Sst: Single-stream temporal action proposals. In *Proceedings of the IEEE Conference on Computer Vision and Pattern Recognition (CVPR)*, 2017.
- [4] F. Caba Heilbron, J. Carlos Niebles, and B. Ghanem. Fast temporal activity proposals for efficient detection of human actions in untrimmed videos. In *Proceedings of the IEEE Conference on Computer Vision and Pattern Recognition (CVPR)*, 2016.
- [5] J. Carreira and A. Zisserman. Quo vadis, action recognition? a new model and the kinetics dataset. *2017 IEEE Conference on Computer Vision and Pattern Recognition (CVPR)*, pages 4724–4733, 2017.
- [6] Y.-W. Chao, S. Vijayanarasimhan, B. Seybold, D. A. Ross, J. Deng, and R. Sukthankar. Rethinking the faster r-cnn architecture for temporal action localization. In *Proceedings of the IEEE Conference on Computer Vision and Pattern Recognition (CVPR)*, 2018.
- [7] J. Choi. Awesome action recognition. <https://github.com/jinwchoi/awesome-action-recognition>.
- [8] X. Dai, B. Singh, G. Zhang, L. S. Davis, and Y. Q. Chen. Temporal context network for activity localization in videos. In *Proceedings of the IEEE International Conference on Computer Vision (ICCV)*, 2017.
- [9] V. Escorcia, F. C. Heilbron, J. C. Niebles, and B. Ghanem. Daps: Deep action proposals for action understanding. In *Proceedings of the European Conference on Computer Vision (ECCV)*, 2016.
- [10] C. Feichtenhofer, A. Pinz, and A. Zisserman. Convolutional two-stream network fusion for video action recognition. In *Proceedings of the IEEE Conference on Computer Vision and Pattern Recognition (CVPR)*, 2016.
- [11] J. Gao, K. Chen, and R. Nevatia. Ctap: Complementary temporal action proposal generation. In *The European Conference on Computer Vision (ECCV)*, 2018.
- [12] J. Gao, Z. Yang, and R. Nevatia. Cascaded boundary regression for temporal action detection. 2017.
- [13] J. Gao, Z. Yang, C. Sun, K. Chen, and R. Nevatia. Turn tap: Temporal unit regression network for temporal action proposals. In *Proceedings of the IEEE International Conference on Computer Vision (ICCV)*, 2017.
- [14] G. Gkioxari and J. Malik. Finding action tubes. In *Proceedings of the IEEE Conference on Computer Vision and Pattern Recognition (CVPR)*, pages 759–768, 2015.
- [15] C. Gu, C. Sun, S. Vijayanarasimhan, C. Pantofaru, D. A. Ross, G. Toderici, Y. Li, S. Ricco, R. Sukthankar, C. Schmid, and J. Malik. AVA: A video dataset of spatio-temporally localized atomic visual actions. *IEEE Conference on Computer Vision and Pattern Recognition (CVPR)*, 2018.
- [16] K. He, G. Gkioxari, P. Dollar, and R. Girshick. Mask r-cnn. In *Proceedings of the IEEE International Conference on Computer Vision*, pages 2961–2969, 2017.
- [17] R. Hou, C. Chen, and M. Shah. Tube convolutional neural network (t-cnn) for action detection in videos. In *The IEEE International Conference on Computer Vision (ICCV)*, 2017.
- [18] R. Hou, R. Sukthankar, and M. Shah. Real-time temporal action localization in untrimmed videos by sub-action discovery. In *Proceedings of the British Machine Vision Conference (BMVC)*, 2017.
- [19] J. Huang, N. Li, T. Zhang, G. Li, T. Huang, and W. Gao. Sap: Self-adaptive proposal model for temporal action detection based on reinforcement learning. In *The Thirty-Second AAAI Conference on Artificial Intelligence (AAAI-18)*, 2018.
- [20] Y.-G. Jiang, J. Liu, A. Roshan Zamir, G. Toderici, I. Laptev, M. Shah, and R. Sukthankar. THUMOS challenge: Action recognition with a large number of classes. <http://csrcv.ucf.edu/THUMOS14/>, 2014.
- [21] E. Jones, T. Oliphant, P. Peterson, et al. SciPy: Open source scientific tools for Python, 2001–.
- [22] D. Joy. Actev scorer. https://github.com/usnistgov/ActEV_Scorer/tree/v0.3.0, 2018.
- [23] V. Kalogeiton, P. Weinzaepfel, V. Ferrari, and C. Schmid. Action tubelet detector for spatio-temporal action localization. In *The IEEE International Conference on Computer Vision (ICCV)*, 2017.
- [24] S. Karaman, L. Seidenari, and A. Del Bimbo. Fast saliency based pooling of fisher encoded dense trajectories. In *ECCV THUMOS Workshop*, 2014.
- [25] A. Karpathy, G. Toderici, S. Shetty, T. Leung, R. Sukthankar, and L. Fei-Fei. Large-scale video classification with convolutional neural networks. In *Proceedings of the IEEE Conference on Computer Vision and Pattern Recognition (CVPR)*, pages 1725–1732, 2014.
- [26] D. P. Kingma and J. Ba. Adam: A method for stochastic optimization. *arXiv preprint arXiv:1412.6980*, 2014.
- [27] T. Lin, X. Zhao, H. Su, C. Wang, and M. Yang. Bsn: Boundary sensitive network for temporal action proposal generation. In *The European Conference on Computer Vision (ECCV)*, 2018.
- [28] M. Marian Puscas, E. Sangineto, D. Culibrk, and N. Sebe. Unsupervised tube extraction using transductive learning and dense trajectories. In *Proceedings of the IEEE international conference on computer vision*, pages 1653–1661, 2015.
- [29] P. Mettes, J. C. van Gemert, and C. G. Snoek. Spot on: Action localization from pointly-supervised proposals. In *European Conference on Computer Vision*, pages 437–453. Springer, 2016.
- [30] D. Millner. Modern hierarchical, agglomerative clustering algorithms, 2011.
- [31] F. Negin and F. Bremond. Human action recognition in videos: A survey. *INRIA Technical Report*, 2016.
- [32] P. Nguyen, T. Liu, G. Prasad, and B. Han. Weakly supervised action localization by sparse temporal pooling network. In *The IEEE Conference on Computer Vision and Pattern Recognition (CVPR)*, 2018.

- [33] NIST. Trecvid 2017 evaluation for surveillance event detection, <https://www.nist.gov/itl/iad/mig/trecvid-2017-evaluation-surveillance-event-detection>.
- [34] S. Oh, A. Hoogs, A. Perera, N. Cuntoor, C.-C. Chen, J. T. Lee, S. Mukherjee, J. Aggarwal, H. Lee, L. Davis, E. Swears, X. Wang, Q. Ji, K. Reddy, M. Shah, C. Vondrick, H. Pirsivash, D. Ramanan, J. Yuen, A. Torralba, A. F. Bi Song, A. Roy-Chowdhury, and M. Desai. A large-scale benchmark dataset for event recognition in surveillance video. In *IEEE Conference on Computer Vision and Pattern Recognition (CVPR)*, 2011.
- [35] D. Oneata, J. Revaud, J. Verbeek, and C. Schmid. Spatio-temporal object detection proposals. In *European conference on computer vision*, pages 737–752. Springer, 2014.
- [36] D. Oneata, J. Verbeek, and C. Schmid. The lear submission at thumos 2014. 2014.
- [37] S. Ren, K. He, R. Girshick, and J. Sun. Faster r-cnn: Towards real-time object detection with region proposal networks. In *Advances in neural information processing systems*, pages 91–99, 2015.
- [38] A. Richard and J. Gall. Temporal action detection using a statistical language model. In *Proceedings of the IEEE Conference on Computer Vision and Pattern Recognition (CVPR)*, 2016.
- [39] S. Saha, G. Singh, and F. Cuzzolin. Amtnet: Action-microtube regression by end-to-end trainable deep architecture. 2017.
- [40] Z. Shou, J. Chan, A. Zareian, K. Miyazawa, and S.-F. Chang. Cdc: Convolutional-de-convolutional networks for precise temporal action localization in untrimmed videos. In *Proceedings of the IEEE Conference on Computer Vision and Pattern Recognition (CVPR)*, pages 1417–1426, 2017.
- [41] Z. Shou, H. Gao, L. Zhang, K. Miyazawa, and S.-F. Chang. Autoloc: Weakly-supervised temporal action localization in untrimmed videos. In *The European Conference on Computer Vision (ECCV)*, 2018.
- [42] Z. Shou, D. Wang, and S.-F. Chang. Temporal action localization in untrimmed videos via multi-stage cnns. In *Proceedings of the IEEE Conference on Computer Vision and Pattern Recognition (CVPR)*, 2016.
- [43] K. Simonyan and A. Zisserman. Two-stream convolutional networks for action recognition in videos. In *Advances in Neural Information Processing Systems*, 2014.
- [44] D. Tran, L. Bourdev, R. Fergus, L. Torresani, and M. Paluri. Learning spatiotemporal features with 3d convolutional networks. In *Proceedings of The IEEE International Conference on Computer Vision (ICCV)*, 2015.
- [45] L. Wang, Y. Qiao, and X. Tang. Action recognition and detection by combining motion and appearance features. 2014.
- [46] H. Xu, A. Das, and K. Saenko. R-c3d: Region convolutional 3d network for temporal activity detection. In *Proceedings of the IEEE International Conference on Computer Vision (ICCV)*, 2017.
- [47] K. Yang, P. Qiao, D. Li, S. Lv, and Y. Dou. Exploring temporal preservation networks for precise temporal action localization. In *The Thirty-Second AAAI Conference on Artificial Intelligence (AAAI-18)*, 2018.
- [48] S. Yeung, O. Russakovsky, G. Mori, and L. Fei-Fei. End-to-end learning of action detection from frame glimpses in videos. In *Proceedings of the IEEE Conference on Computer Vision and Pattern Recognition (CVPR)*, 2016.
- [49] J. Yuan, B. Ni, X. Yang, and A. A. Kassim. Temporal action localization with pyramid of score distribution features. In *Proceedings of the IEEE Conference on Computer Vision and Pattern Recognition (CVPR)*, 2016.
- [50] Z.-H. Yuan, J. C. Stroud, T. Lu, and J. Deng. Temporal action localization by structured maximal sums. In *Proceedings of the IEEE Conference on Computer Vision and Pattern Recognition (CVPR)*, 2017.
- [51] J. Yue-Hei Ng, M. Hausknecht, S. Vijayanarasimhan, O. Vinyals, R. Monga, and G. Toderici. Beyond short snippets: Deep networks for video classification. In *Proceedings of the IEEE Conference on Computer Vision and Pattern Recognition (CVPR)*, pages 4694–4702, 2015.
- [52] C. Zach, T. Pock, and H. Bischof. A duality based approach for realtime tv-l 1 optical flow. In *Joint Pattern Recognition Symposium*, pages 214–223. Springer, 2007.
- [53] Y. Zhao, Y. Xiong, L. Wang, Z. Wu, X. Tang, and D. Lin. Temporal action detection with structured segment networks. In *Proceedings of the IEEE International Conference on Computer Vision (ICCV)*, 2017.
- [54] H. Zhu, R. Vial, and S. Lu. Tornado: A spatio-temporal convolutional regression network for video action proposal. In *Proceedings of the IEEE Conference on Computer Vision and Pattern Recognition (CVPR)*, pages 5813–5821, 2017.